Design Method of Cooling Structure Considering Load Fluctuation of High-power Wireless Power Transfer System

Jun-ichi Itoh
Dept. of Electrical, Electronics, and Information Engineering
Nagaoka University of Technology
Nagaoka, Japan
itoh@vos.nagaokaut.ac.jp

Kosuke Mizoguchi
Dept. of Electrical, Electronics, and Information Engineering
Nagaoka University of Technology
Nagaoka, Japan
nagaoka_mizo@stn.nagaokaut.ac.jp

Le Hoai Nam
Dept. of Electrical, Electronics, and Information Engineering
Nagaoka University of Technology
Nagaoka, Japan
lehoainam@stn.nagaokaut.ac.jp

Keisuke Kusaka
Dept. of Electrical, Electronics, and Information Engineering
Nagaoka University of Technology
Nagaoka, Japan
kusaka@vos.nagaokaut.ac.jp

***Abstract*— This paper proposes a thermal design method for transmission coils with thermally conductive plastic plates considering load fluctuation of high-power wireless power transfer (WPT) systems. The high power transmission may cause melting of an insulation coating film of litz wires due to the heat generation of the windings and cores. For this reason, a cooling structure for the transmission coils is required. As the cooling structure, thermally conductive plastic plates with high thermal conductivity and resistivity are inserted between the core and the aluminum plates for an improvement of heat transfer. By representing the cooling structure as a thermal equivalent circuit, it facilitates a thermal design that takes into account load fluctuations. The thermal equivalent circuit is composed of a two-stage ladder circuit divided into the WPT system part and a cooling part. The peak temperature and the maximum allowable loss of load fluctuation are derived by simplifying the two-stage ladder circuit. In addition, the thickness of the thermally conductive plastic plates is designed by the design flowchart for the 15-kW WPT system.**

Keywords*— *Wireless power transfer, thermally conductive plastic, high-power, load fluctuation, thermal equivalent circuit

I. INTRODUCTION

Recently, high-power WPT systems have been actively studied [1]. A wireless power transfer (WPT) provides convenience because the power is fed without metal contacts and connectors. Thus, WPT is superior to wired power supply systems, and its application in various fields is expected. For the applications requiring high power such as electric vehicles and construction machines [2–3], the design to achieve high power is considered. As an example, the WPT system for large-capacity excavator has been proposed [3]. Currently, the development of the WPT system with an input power of 3.3 or 7.7 kW is moving towards a commercial for light-duty vehicles with a standardization. Meanwhile, the transmission power of the bus is much higher than the light-duty electric vehicles [4–5].

However, there is a problem that the ferrite cores and the windings in the high-power WPT system generate heat due to copper loss and iron loss [6]. In particular, the temperature rise of the litz wire may melt the insulating film of the litz wire, eventually causing insulation breakdown between the windings. Thus, a cooling structure is required to suppress the heat of the high-power WPT system. Thermal design is typically performed by simulation using the finite element method (FEM) [7]. The optimal solution is unclear since the FEM requires various conditions such as mesh and heat transfer conditions. In addition, the load of the WPT system is assumed to be a charger or a motor for construction machines. For this reason, the WPT system repeats the operation and standby. When temperature analysis is performed using FEM for repeat operations, the analysis may take a long time.

This paper proposes a thermal design method considering load fluctuations of a high-power WPT system with a cooling structure using thermally conductive plastic plates. Considering the cooling structure with the thermal equivalent circuit, it is possible to easily perform thermal design even when the load fluctuates. Moreover, the thermal design with the thermal equivalent circuit shortens the thermal analysis time. By expressing the system by the thermal equivalent circuit, the thermal design is optimized by solving the thermal equivalent circuit with a differential equation. The applied cooling structure for this paper consists of winding, ferrite core, thermally conductive plastic plates, and aluminum plates. Each material is represented by a thermal resistance and a heat capacity on the thermal equivalent circuit. The equivalent circuit consists of a two-stage ladder circuit divided into the WPT system part and the cooling part. In order not to exceed the limitation on temperature, the maximum loss must be determined from the steady peak temperature of the two-stage ladder circuit. However, it is mathematically difficult to derive the peak temperature of the two-stage ladder circuit. Thus, the peak temperature is obtained by approximating the two-stage ladder circuit. The allowable loss in order to make the coils under the temperature limitation is derived from the peak temperature. Then, the cooling structure is designed by electromagnetic field analysis. The proposed flowchart adjusts the thickness of the thermally conductive plastic to bring the cooling structure below the maximum loss.

978-1-7281-3153-5/19/$31.00 ©2019 IEEE

II. WIRELESS POWER TRANSFER SYSTEM FOR HIGH-POWER EV CHARGER

A. System configuration

Figure 1 shows a circuit configuration of the WPT system. The system consists of a single-phase inverter on the primary side and a rectifier on the secondary side. In this system, the series resonance compensation is applied to the primary side, whereas the parallel resonance compensation to the secondary side, i.e. SP resonance compensation, in order to supply a constant voltage to the battery charging system. Thus, the load voltage is constant regardless of the load fluctuation when a constant voltage is applied to the primary coil. As a result, it is possible to obtain the maximum efficiency at the designed output power.

B. Design of WPT system

Figure 2 shows the equivalent circuit of the WPT system. Table I shows the specifications of the WPT system. In this system, as one of the example, an output power of 15 kW is assumed. The equivalent resistance of the load-side rectifier is replaced by the equivalent series resistance R_{eq} [8]. The equivalent load resistance R_{eq} of the full-bridge rectifier is expressed by (1).

$$R_{eq} = \frac{\pi^2}{8}\frac{V_{2,DC}^2}{P_2} \tag{1}$$

The self-inductances of the primary side coil and the secondary side coil are designed to be equal to the impedance of the equivalent load resistance R_{eq} and the excitation inductance [9]. As a result, it is possible to obtain the maximum efficiency at the designed output power. The self-inductances of the primary side coil and the secondary side coil are expressed by (2),(3).

$$L_2 = \frac{R_{eq}}{\omega_0}\frac{k}{\sqrt{1+k^2}} \tag{2}$$

$$L_1 = L_2\left(\frac{8}{\pi^2 k}\frac{V_{1.DC}}{V_{2,DC}}\right)^2 \tag{3}$$

Then, the resonant capacitors are determined according to (4) and (5) so that the power factor stand from the primary side is unity.

$$C_1 = \frac{1}{\omega_0^2 L_1(1-k^2)} \tag{4}$$

$$C_2 = \frac{1}{\omega_0^2 L_2} \tag{5}$$

C. Cooling structure of WPT system

Figure 3 shows the structures of two cooling structures. Fig. 3(a) shows the conventional cooling structure using only the aluminum plates [10]. This structure transfers heat directly to the aluminum plates. However, eddy current loss occurs in the cooling aluminum plates. In particular, when the core is placed close to the aluminum plates, eddy currents are generated in the aluminum plates, causing the decrease in the transmission efficiency and the heat generation of the

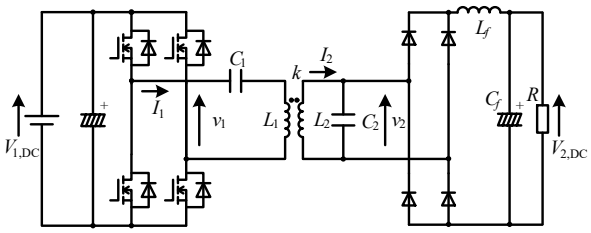

Fig. 1. WPT system with SP resonance compensation.

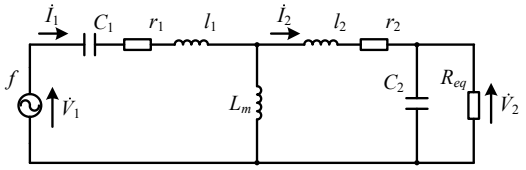

Fig. 2. Equivalent circuit of the WPT system.

TABLE I. DESIGN PARAMETERS OF THE WPT SYSTEM.

	Symbol	Value
Primary DC voltage	$V_{1,DC}$	640 V
Secondary DC voltage	$V_{2,DC}$	640 V
Rated Output power	P_{out}	15 kW
Switching frequency	f	20 kHz
Coupling coefficient	k	0.4
Primary inductance	L_1	409 μH
Secondary inductance	L_2	100 μH
Primary capacitance	C_1	184 nF
Secondary capacitance	C_2	636 nF

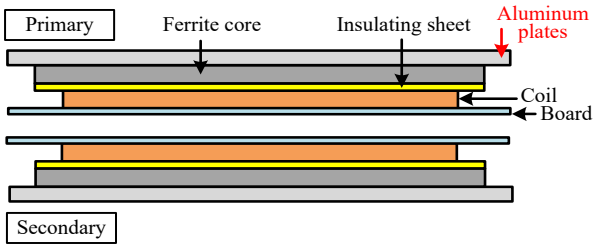

(a) Conventional cooling structure: Aluminum plates (worst condition).

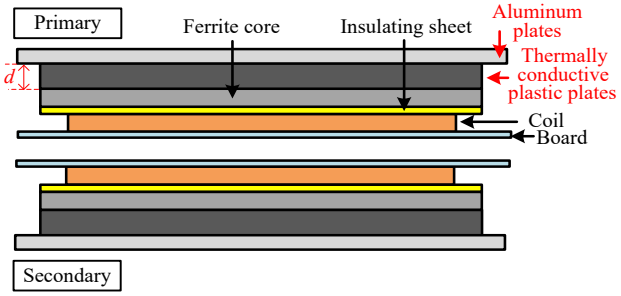

(b) Proposal cooling structure: Aluminum plates + Thermally conductive plastic plates

Fig. 3. Structure of cooling systems.

aluminum plates themselves. Fig. 3 (b) shows the proposed cooling structure using the thermally conductive plastic plates. The thermally conductive plastic plates, which are made of a material with a high resistivity of 2.2 × 10^6 Ωm and high thermal conductivity of 21 W/mK [11], are inserted between the cores and the aluminum plates. Meanwhile, it is difficult to transfer the heat from the heat source to the outside when only the thermally conductive plastic plates are used. Thus, the proposed structure also uses the aluminum plates, which have a high thermal conductivity of 138 W/mK. The proposed cooling method suppresses the eddy current loss generated in the aluminum plates while cooling the primary and secondary coils. In addition, the eddy current loss is reduced by increasing the thickness of the thermally conductive plastic plates.

D. Thermal equivalent circuit

Figure 4 shows a thermal equivalent circuit in which the proposed structure is divided into the WPT system part and a cooling part. The thermal equivalent circuit is easily possible to design even when the load fluctuates repeatedly. When the thermal equivalent circuit is solved in consideration of the heat capacity, the cycle time to the steady temperature is derived. In addition, the thermal design is optimized by solving the differential equations of the thermal equivalent circuit. The thermal equivalent circuit is a two-stage ladder circuit composed of the WPT system part and a cooling part The operating condition of the WPT system applies the total loss Q [W], and the standby condition applies the heat source as 0W. Total loss Q [W] consists losses from windings, core, and aluminum plate. The heat capacity of the winding and ferrite core is C_1 [J/K], the thermal resistance is R_1 [K/W], and the temperature is T_1 [°C]. The heat capacity of thermally conductive plastic plates and aluminum plates is C_2 [J/K], the thermal resistance is R_2 [K/W], and the temperature is T_2 [°C]. The equation for T_1 and T_2 is expressed by nodal equations. The equations for operating conditions T_1 and T_2 is expressed as (6).

$$\begin{cases} Q = C_1 \dfrac{dT_1}{dt} + \dfrac{T_1 - T_2}{R_1} \\ \dfrac{T_1 - T_2}{R_1} = C_2 \dfrac{dT_2}{dt} + \dfrac{T_2}{R_2} \end{cases} \tag{6}$$

Equation (6) is Laplace transform, and the temperature at the start of operation is expressed as (7).

$$\begin{cases} \dfrac{Q}{s} = sC_1T_1(s) + \dfrac{T_1(s) - T_2(s)}{R_1} \\ \dfrac{T_1(s) - T_2(s)}{R_1} = sC_2T_2(s) + \dfrac{T_2(s)}{R_2} \end{cases} \tag{7}$$

Each $T_1(s)$ and $T_2(s)$ are derived from (7). When inverse Laplace transform is performed, $T_1(t)$ and $T_2(t)$ are obtained. Except for the start of the operation, it is necessary to apply the initial temperature in the heat capacity. The initial temperature of the winding and ferrite core is T_{01}. The initial temperature of the thermally conductive plastic plates and aluminum plates are T_{02}. Considering the initial temperatures T_{01} and T_{02} in (6), the result of Laplace transform is expressed as (8).

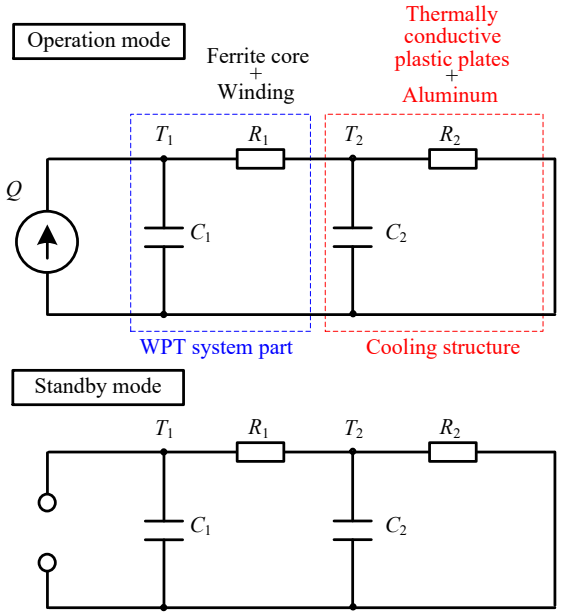

Fig. 4. Thermal equivalent circuit corresponding to load fluctuation of the WPT system.

$$\begin{cases} \dfrac{Q}{s} = C_1\left(sT_1(s) - T_{01}\right) + \dfrac{T_1(s) - T_2(s)}{R_1} \\ \dfrac{T_1(s) - T_2(s)}{R_1} = C_2\left(sT_2(s) - T_{02}\right) + \dfrac{T_2(s)}{R_2} \end{cases} \tag{8}$$

Each $T_1(s)$ and $T_2(s)$ are derived from (8). When inverse Laplace transform is performed, temperature rise $T_1(t)$ and $T_2(t)$ from the initial temperature are obtained.

The temperature of the WPT system during a standby condition drops because the total loss Q [W] in the standby condition is 0 W. The loss in Fig. 4 is opened. The temperature during the standby condition is expressed as (9).

$$\begin{cases} 0 = C_1 \dfrac{dT_1}{dt} + \dfrac{T_1 - T_2}{R_1} \\ \dfrac{T_1 - T_2}{R_1} = C_2 \dfrac{dT_2}{dt} + \dfrac{T_2}{R_2} \end{cases} \tag{9}$$

Considering the initial temperatures T_{01} and T_{02} in (9), the result of Laplace transform is expressed as (10).

$$\begin{cases} 0 = C_1\left(sT_1(s) - T_{01}\right) + \dfrac{T_1(s) - T_2(s)}{R_1} \\ \dfrac{T_1(s) - T_2(s)}{R_1} = C_2\left(sT_2(s) - T_{02}\right) + \dfrac{T_2(s)}{R_2} \end{cases} \tag{10}$$

Each $T_1(s)$ and $T_2(s)$ are derived from (10). When inverse Laplace transform is performed, temperature drop $T_1(t)$ and $T_2(t)$ from the initial temperature are obtained. From the above, the temperature rise and drop by the load fluctuation is calculated by the above equation. In other words, the time to reach the peak temperature is calculated.

E. Derivation of peak temperature and allowable loss

Figure 5 shows a thermal equivalent circuit with an approximation of the peak temperature. Figure 6 shows an

explanatory diagram for deriving the peak temperature. If the operation continues for a long time until the steady temperature is reached, the peak temperature is determined. However, the above method of obtaining the peak temperature takes a long time. Thus, it is necessary to derive an approximate expression for the peak temperature. Furthermore, it is necessary to design the heat by deriving the maximum allowable loss of the cooling structure. The maximum allowable loss is derived from the peak temperature. The thermal equivalent circuit for obtaining the peak temperature assumes that R_2 and C_2 parts on the secondary side of the two-stage ladder circuit are the average temperature T_2. The thermal equivalent circuit in Fig. 5 is expressed as (11).

$$\begin{cases} Q = C_1 \dfrac{dT_1}{dt} + \dfrac{T_1 - T_2}{R_1} \\ 0 = C_1 \dfrac{dT_1}{dt} + \dfrac{T_1 - T_2}{R_1} \end{cases} \tag{11}$$

The peak temperature is obtained from the simultaneous equations of temperature rise and drop in the steady-state. The Laplace transform of (11) is expressed as (12).

$$\begin{cases} \dfrac{Q}{s} = C_1\left(sT_1(s) - T_{01}\right) + \dfrac{T_1(s)}{R_1} - \dfrac{T_2}{sR_1} \\ 0 = sC_1T_1(s) - C_1T_0 + \dfrac{T_1(s)}{R_1} - \dfrac{T_2}{sR_1} \end{cases} \tag{12}$$

The temperature rise and drop of $T_1(s)$ is express as (13) from (12) with inverse Laplace transform.

$$\begin{cases} T_1(t) = T_2 + QR_1 - \exp\left(-\dfrac{t}{C_1R_1}\right)\left(T_2 - T_0 + QR_1\right) \\ T_1(t) = T_2 + \exp\left(-\dfrac{t}{C_1R_1}\right)\left(T_0 - T_2\right) \end{cases} \tag{13}$$

As shown in Fig. 6, when the temperature after t_a is the peak temperature T_{peak} and the temperature after t_b is the lower limit value T_0, the temperature expressed as (14).

$$\begin{cases} T_1(t_a) = T_{peak} = T_2 + QR_1 - \exp\left(-\dfrac{t_a}{C_1R_1}\right)\left(T_2 - T_0 + QR_1\right) \\ T_1(t_b) = T_0 = T_2 + \exp\left(-\dfrac{t_b}{C_1R_1}\right)\left(T_{peak} - T_2\right) \end{cases} \tag{14}$$

Solving for T_{peak} from the simultaneous equations in (14), the approximate equation for peak temperature is expressed as (15).

$$A = \exp\left(-\frac{t_a}{C_1R_1}\right), B = \exp\left(-\frac{t_b}{C_1R_1}\right)$$

$$T_{peak} = \frac{T_2(1 - AB) + QR_1(1 - A)}{1 - AB} \tag{15}$$

The approximation formula for peak temperature is extremely precise [12]. The maximum allowable loss is obtained by the deformation of (15). The maximum allowable loss Q_{max} is expressed as (16).

$$Q_{max} = \frac{T_{peak}(1 - AB) - T_2(1 - AB)}{R_1(1 - A)} \tag{16}$$

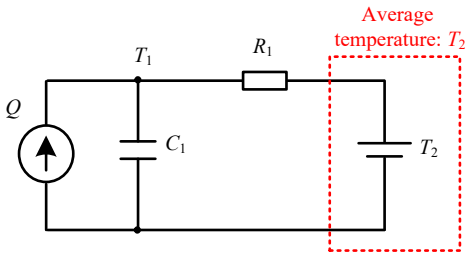

Fig. 5. Thermal equivalent circuit for determining peak temperature.

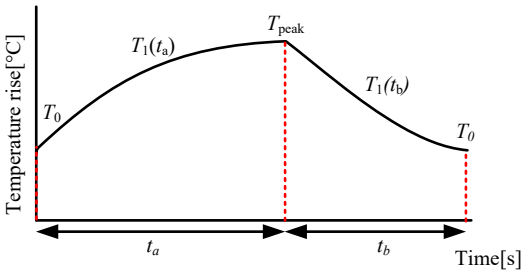

Fig. 6. Derivation of peak temperature on steady-state.

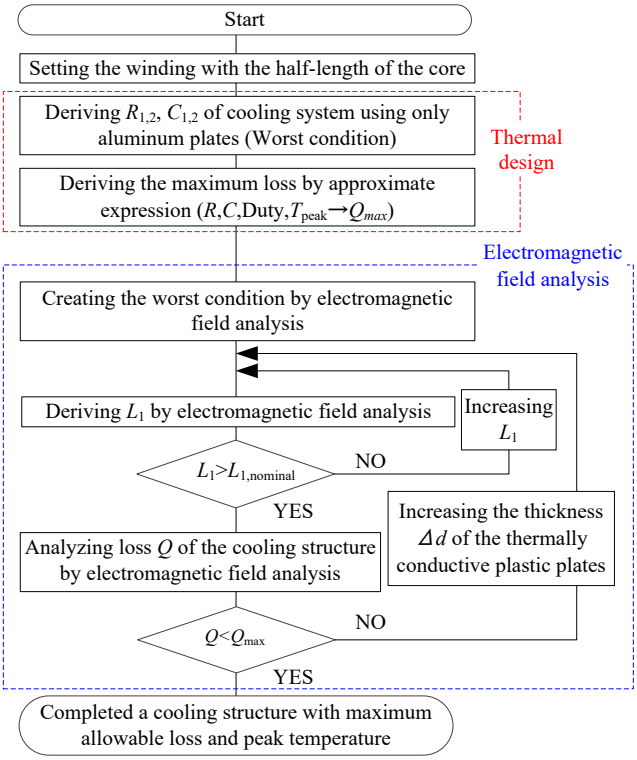

Fig. 7. Flowchart of thermal design.

F. Thermal design

Figure 7 shows the flowchart of the thermal design for the WPT system with the proposed cooling structure. In order to design the cooling structure, thermal analysis, and electromagnetic field analysis are used for the evaluation of the cooling performance. The advantage of the proposed design flow is a one-loop thermal analysis. Thus, there is no

need to perform thermal analysis many times. According to the flowchart of Fig. 7, the thickness of the thermally conductive plastic plates in the proposed cooling structure is determined. At the first, the model with aluminum plates, which directly connected to the core, is analyzed. The thickness of the thermally conductive plastic plates is set to 0-mm. In other words, it is as same as the conventional structure shown in Fig. 3. This cooling structure assumes that the ferrite winding area is half of the core. Heat capacity and thermal resistance are taken from the cooling model and taken into account in the thermal equivalent circuit. The maximum allowable loss of the cooling structure is derived from conditions such as peak temperature. The next step is to model the cooling structure of the worst condition with electromagnetic field analysis. The inductance value of the primary winding is analyzed with the electromagnetic field analysis. If the inductance value exceeds the nominal value, the loss analysis of the cooling structure is analyzed by electromagnetic field analysis. If the analyzed loss exceeds the maximum allowable loss, the thickness of the thermally conductive plastic plates is increased in order to reduce the eddy current loss. If the maximum allowable loss is not reached, the cooling structure that lowers the winding temperature below the allowable temperature is determined.

III. Thermal Analysis and Loss Analysis

A. Thermal analysis

The primary side and secondary current of $k = 0.4$ are $I_1 = 37.3$ A, $I_2 = 85.6$ A, and the gap of the WPT system is 100-mm. This condition is not changed even if the cooling structure changes. In this condition, the loss on the primary side is larger than the secondary side due to a large number of turns and winding resistance. Thus, the thermal design targets the primary WPT system.

Table II shows the density, specific heat, volume, and heat capacity of each part of the WPT system. Table III shows the thickness, thermal conductivity, thermal transfer area, and thermal resistance of each material. The heat capacity of each part is expressed by (17) using the density ρ [kg/m^3], specific heat c [J/(kg·K)], and volume V [m^3] in Table III. The heat capacity and thermal resistance are calculated from the worst condition structure.

$$C = \rho c V \tag{17}$$

The thermal resistance R [K/W] of each material is expressed by (18) using the thickness L [m], thermal transfer surface A [m^2], and thermal conductivity K [W/(m·K)] in Table III.

$$R = \frac{L}{KA} \tag{18}$$

There is a difference in the heat transfer area between the winding and the core. Thus, the thermal resistance R'[K/W] when heat spreads in the thickness direction and the surface direction is expressed as (19).

$$R' = \frac{L}{ka(2L + a)} \tag{19}$$

By the above formula, the thermal conductivity and heat capacity of the worst condition shown in Fig. 4 are $R_1 = 0.157$ K/W and $C_1 = 6299$ J/K, $R_2 = 0.0405$ K/W, and $C_2 = 5849$ J/K.

TABLE II. Thermal Capacity of Each Material.

	Density [kg/m^3]	Specific heat [J/(kg·K)]	Volume [m^3]	Thermal capacity [J/K]
Copper (winding)	8960	380	255.6×10^{-6}	870.3
Ferrite core	4800	600	1998×10^{-6}	5753.1
Aluminum	2680	900	2425×10^{-6}	5849.1
Thermally conductive plastic	1490	950	-	-

TABLE III. Thermal Resistance of Each Material.

	Thickness [m]	Thermal conductivity [W/mK]	Thermal transfer area [m^2]	Thermal resistance [K/W]
Primary winding	0.004	403	0.04	0.00025
Ferrite core	0.01	5	0.20	0.0154
Aluminum	0.01	138.3	0.24	0.0003
Silicon grease	-	0.84	-	0.0402
Osculating plane	-	-	-	0.0755
Insulating sheet	0.0002	0.2	0.20	0.0050
Thermally conductive plastic	-	21	0.20	-

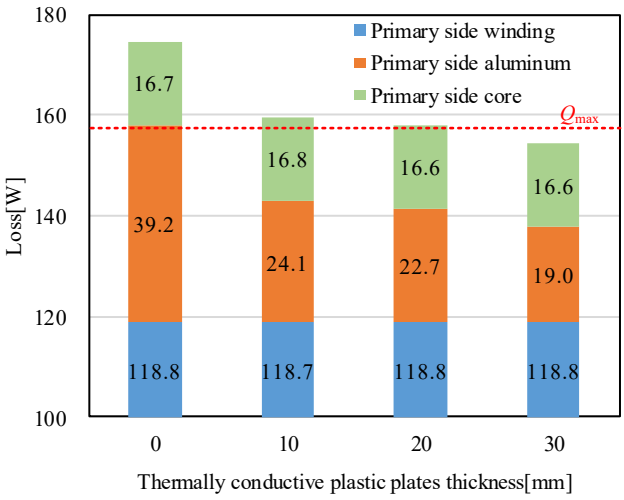

Fig. 8. Total loss due to the thickness of thermally conductive plastic plates.

Load fluctuation is designed to operate and standby in a 30-minute cycle. The duty ratio of this paper is 90%. This duty ratio is the operation time in one cycle time. In other words, it operates for 27-minutes in 30-minutes, and standby for 3-minutes. Under these conditions, to suppress the temperature rise of the WPT system below 30°C, the allowable power loss is 158.0 W by (16). Thus, the loss from the cooling structure must be less than this maximum allowable loss.

B. Loss analysis

Figure 8 shows an analyzed power loss with the different thickness of the thermally conductive plastic plates. The power loss is lower than the maximum allowable loss when the thickness is larger than 30-mm. As a result, the eddy

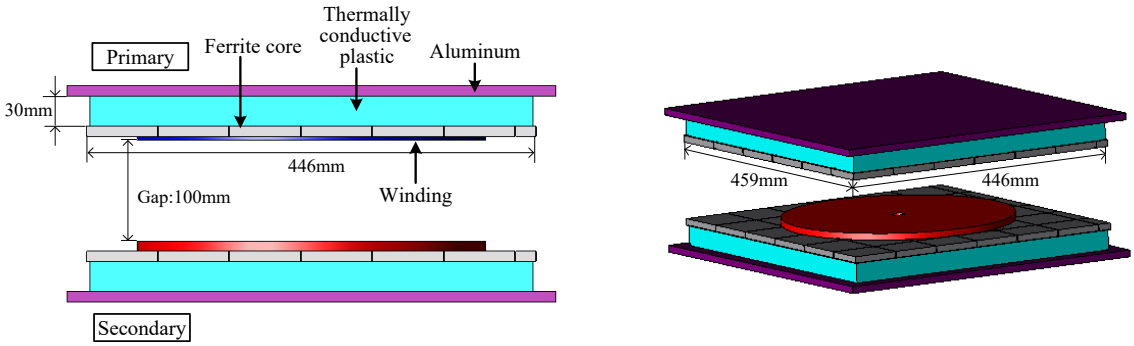

Fig. 9. Cooling structure with less than maximum allowable loss by electromagnetic field analysis.

current loss is reduced by 51.5% and the total loss is suppressed to 154.3 W.

Figure 9 shows the cooling structure with the 30-mm thermally conductive plastic plates. The thickness of the thermally conductive plastic plates is 30-mm, and it is placed between the aluminum plates and the core. The primary winding is 42-turns and the inductance value is 421μH.

IV. Conclusion

This paper proposed a thermal design method considering load fluctuations of a high-power WPT system with a cooling structure using thermally conductive plastic plates. Considering the cooling structure with the thermal equivalent circuit, it is possible to easily perform thermal design even when the load fluctuates. Moreover, the thermal design with the thermal equivalent circuit shortens the thermal analysis time. By expressing the system by the thermal equivalent circuit, the thermal design is optimized by solving the thermal equivalent circuit with a differential equation. The proposed flowchart is designed for the thickness of the thermally conductive plastic plates that is below the maximum allowable loss. The maximum allowable loss should not exceed 158.0 W. As a result, eddy current loss is reduced by 51.5% and the total loss is suppressed to 154.3 W when the thickness of the thermally conductive plastic plates is 30-mm.

In the future, we will verify and evaluate the proposed design method by prototype experiments.

References

[1] Keisuke Kusaka, Jun-ichi Itoh, “Development Trends of Inductive Power Transfer Systems Utilizing Electromagnetic Induction with Focus on Transmission Frequency and Transmission Power,” IEEJ Journal Industry Applications, vol. 6, no. 5, pp. 328-339, 2017.

[2] Mostak Mohammad, Seungdeog Choi, Md Zakirul Islam, Sangshin Kwak, Jeihoon Baek, “Core Design and Optimization for Better Misalignment Tolerance and Higher Range of Wireless Charging of PHEV,” IEEE Trans. Transportation Electrification, vol. 3, no. 2, pp. 445-453, 2017.

[3] Keisuke Kusaka, Kent Inoue, and Jun-ichi Itoh, “Inductive Power Transfer System for an Excavator by considering Large Load Fluctuation,” IEEJ Journal Industry Applications, vol. 8, no. 3, pp. 413-420, 2019.

[4] Chunting Chris Mi, Giuseppe Buja, Life Fellow, Su Y. Choi, Chun T. Rim, “Modern Advances in Wireless Power Transfer Systems for Roadway Powered Electric Vehicles,” IEEE Trans. Industrial Electron., vol. 63, no. 10, pp.6533-6545, 2016.

[5] J. Shin, S. Shin, Y. Kim, S. Ahn, S. Lee, G. Jung, S. Jeon, D. Cho, “Design and Implementation of Shaped Magnetic-Resonance-Based Wireless Power Transfer System for Roadway-Powered Moving Electric Vehicles,” IEEE Trans. Industrial Electron., vol. 61, no. 3, pp. 1179-1192, 2014.

[6] Kosuke Mizoguchi, Keisuke Kusaka, Jun-ichi Itoh, “Evaluation of Cooling Method for Wireless Power Transfer System using Thermally Conductive Plastics,” Technical Committee on Semiconductor Power Converter , SPC-19-044, MD-19-044, 2019.

[7] B. Dong, K. Wang, B. Han and S. Zheng, "Thermal Analysis and Experimental Validation of a 30 kW 60000 r/min High-Speed Permanent Magnet Motor With Magnetic Bearings," IEEE Access, vol. 7, pp. 92184-92192, 2019.

[8] R. L. Steigerwald, “A comparison of half-bridge resonant converter topologies,” IEEE Trans. Power Electron., vol. 3, no. 2, pp. 174-182, 1988.

[9] Roman Bosshard, Johann Walter Kolar, Jonas Muhlethaler, Ivica Stevanovic, Bernhard Wunsch, Fransisco Canales, “Modeling and η-α-Perato Optimization of Inductive Power Transfer Coils for Electric Vehicles,” IEEE Journal Emerging and Selected Topics in Power Electron., vol. 3, no. 1, pp. 50-64, 2015.

[10] Tomohiro Yamanaka, Itaru Fujita, Yasuyoshi Kaneko, Shigeru Abe, Tomio Yasuda, “Cooling Structure for Large Capacity H-shaped Core Contactless Power Transformers for Electric Vehicles,” IEEJ Trans. Industry Applications, vol. 134, no. 3, pp. 370-375, 2014.

[11] Yamashita Materials Corporation, “Thermal Conductive Plastic,” http://www.yamashita-net.co.jp/english/

[12] Kosuke Mizoguchi, Keisuke Kusaka, Jun-ichi Itoh, “Design Method of Cooling Structure Considering Load Fluctuation of High-power Wireless Power Transmission System,” Technical Committee on Semiconductor Power Converter , SPC-19-123, MD-19-089, 2019.